Refining Sigal et al.'s Model of Cancer Treatments and Heterogeneous Tumor Growth in "Mathematical Modeling of Cancer Stem Cell-Targeted Immunotherapy" to Exhibit Gompertzian Growth

Catherine Feng
Harvard College '27

Tumors are typically heterogeneous, consisting of multiple cell types. A small but aggressive subset are cancer stem cells (CSCs), which are closely related to tumor growth and resistance, making them critical targets for therapeutic intervention. Traditional therapies like chemotherapy often fail to eradicate CSCs, necessitating targeted treatments like immunotherapy. While the interactions of different types of cancer and immune cells, immunotherapy, and chemotherapy have been studied experimentally, mathematical models are needed to better understand why certain treatments fail and how to improve cancer treatment. In this manuscript, I replicate and expand upon a mathematical model developed by Sigal et al. (2019) that employs a system of seven ordinary differential equations (ODEs) to simulate the effects of immunotherapy and chemotherapy on tumors containing both CSCs and non-CSCs (nCSCs). The model incorporates two types of immune cells involved in promising immunotherapies and antitumor response: dendritic cells (DCs) and cytotoxic T-cells (CTCs). I modify the original model by introducing a Gompertzian growth term to better capture long-term tumor growth as the tumor approaches its carrying capacity, addressing the model's current limitations. Future work includes refining parameter values and extending the model to account for tumors composed solely of CSCs or nCSCs. This modified model has the potential to provide valuable insights into the potential efficacy and optimal timing of cancer treatments.

Introduction

Most tumors are heterogeneous, comprising multiple types of tumor cells (Turner & Kohandel, 2012). Cancer stem cells (CSCs) are one such type that are closely related to poor patient outcomes, including tumor growth, resistance, metastasis, and recurrence, making them an important and attractive target of study and treatment.

CSCs are a class of tumor cells able to perpetually self-renew and differentiate into other types of cancer cells. While CSCs typically make up under 10% of cells in a tumor, they exhibit fast and aggressive growth. Moreover, CSCs are resistant to traditional therapies like chemotherapy or radiotherapy. Therefore, immunotherapy, where the patient's own immune system is used to target tumor cells in a highly specific manner, has gained prominence as a treatment. Because of the specificity of this treatment, immunotherapy can even be used to directly target CSCs (Wu et al., 2023).

While the interactions of different types of cancer cells, immunotherapy, and traditional therapeutic methods like chemotherapy have been extensively studied experimentally, mathematical models are needed to better understand why certain treatments fail and how to improve cancer treatment. Previous work modeling the interactions between cancer and immune cells treat tumors as a homogeneous population, overlooking the significant differences between CSCs and non-CSCs (nCSCs, which have less or no capacity for self renewal or differentiation) (Robertson-Tessi et al., 2012; Wilkie & Hahnfeldt, 2013). More recent models distinguish between CSCs and nCSCs (Goldman et al., 2015) and consider their interactions with chemotherapy and the immune system (Mpekris et al., 2017, 2020). However, few address the combined effects of chemotherapy and immunotherapy in a comprehensive framework. Since CSCs play a significant role in driving tumor progression, developing a model that considers the interactions between CSCs, nCSCs, and immune cells under chemotherapy and immunotherapy is crucial for advancing our understanding of cancer treatment.

In a 2019 paper by Sigal et al. entitled "Mathematical Modeling of Cancer Stem Cell-Targeted Immunotherapy," the authors used 7 ordinary differential equations (ODEs) to model the effects of using immunotherapy and chemotherapy alone or in combination on tumors arising from CSCs and nCSCs. Using this model, they tried to seek the best treatment plan.

The authors chose two parts of the immune system involved in promising immunotherapy treatments: dendritic cells (DCs) and cytotoxic T-cells (CTCs) (Sigal et al., 2019). These cells are a critical component of antitumor response, with DCs taking up cancer antigens and presenting them to CTCs so they can recognize and kill tumors (Jhunjhunwala et al., 2021).

In treatments involving these cells, immature DCs are taken from a patient and activated with tumor antigens to make them present antigens specific to CSCs (which express antigens similar to normal stem cells) or nCSCs (Galassi et al., 2021). These mature DCs were then reintroduced into the patient to interact with and activate naive CTCs to target cancer cells that exhibit the same antigen. However, as a consequence, mature DCs presenting antigens can also be targeted and killed by activated CTCs (Ma et al., 2012). While there are mechanisms protecting mature DCs from such attacks, Sigal et al. (2019) make the simplifying assumptions that activated CTCs will only target mature DCs and tumor cells with the same type of antigen, and choose not to account for these protecting mechanisms.

Based on these factors, Sigal et al. (2019) created a system of 7 ODEs (Equation 1) modeling the effects of the above immunotherapy treatments and chemotherapy. The system modeled the populations of CSCs, nCSCs, activated CSC-specific CTCs, activated nCSC-specific CTCs, mature CSC-specific DCs, and mature nCSC-specific DCs. These dependent variables were denoted as S, P, T_S, T_P, D_S, and D_P, respectively. C was used to denote the concentration of chemotherapeutic agents:

$$\frac{dS}{dt} = \alpha_S S + \rho_{PS} P - \rho_{PS} S - \beta_S S T_S - \delta_S S - \Gamma_S S C$$

$$\frac{dP}{dt} = \alpha_P P + \alpha_{SP} S + 2\rho_{SP} S - \rho_{PS} P - \beta_P P T_P - \delta_P P - \Gamma_P P C$$

$$\frac{dT_S}{dt} = K_{T_S} T_S{}^n \frac{D_S}{S_{T_S}+D_S} - \delta_{T_S} T_S$$

$$\frac{dT_P}{dt} = K_{T_P} T_P{}^n \frac{D_P}{S_{T_P}+D_P} - \delta_{T_P} T_P \quad \textbf{(1)}$$

$$\frac{dD_S}{dt} = \gamma_{D_S} D S - \beta_{D_S} D_S T_S - \delta_{D_S} D_S$$

$$\frac{dD_P}{dt} = \gamma_{D_P} D P - \beta_{D_P} D_P T_P - \delta_{D_P} D_P$$

$$\frac{dC}{dt} = -e_C C$$

Descriptions of the parameters and possible values can be found in **Table 1**.

Parameter	Description	Value
Host-specific		
α_S	reproduction rate of CSCs	0.14 - 0.76 day^{-1}
α_{SP}	production of nCSCs through asymmetrical division of CSCs	0.4 - 6 day^{-1}
α_P	reproduction rate of nCSCs	0 - 0.8 day^{-1}
ρ_{PS}	conversion rate of nCSCs to CSCs	fit as needed to keep %CSCs within 1-10%
ρ_{SP}	conversion rate of CSCs to nCSCs	0 - 0.76 day^{-1}
δ_S	natural death rate of CSCs	0 - 0.25 day^{-1}
δ_P	natural death rate of nCSCs	0 - 0.39 day^{-1}
δ_{D_S}, δ_{D_P}	natural death rate of CSC- or nCSC-specific DCs	0.2 - 0.8 day^{-1}
Non-host-specific		
β_S, β_P	death rate of CSCs or nCSCs due to CTCs	6.2 x 10^{-8} $(aCTCs \cdot day)^{-1}$
$\kappa_{T_S} T_S^n$, $\kappa_{T_P} T_F^n$	saturated activation rate of CTCs by mDCs multiplied by the population of CSC- or nCSC-specific naïve CTCs	4.5 x 10^4 (aCTCs/μL)/day
s_{T_S}, s_{D_P}	mDC value at which CTC activation rate is half of its maximum possible value	2.5 x 10^4 mDCs/μL
δ_{T_S}, δ_{T_P}	natural death rate of CSC- or nCSC-specific CTCs	0.02 day^{-1}
$\Upsilon_{D_S} D$, $\Upsilon_{D_P} D$	maturation rate of DCs due to consumption of cancer cells multiplied by the constant D (population of immature DCs)	0.0063 (mDCs/μL) / (day · cancer cell / μL)
β_{D_S},β_{D_P}	death rate of CSC- or nCSC-specific DCs due to CTCs	6.2 x 10^{-8} $(aCTCs/\mu L \cdot day)^{-1}$
Drug-specific		
Γ_S	rate of killing of CSCs by the chemotherapeutic agent	7.8 - 14 x 10^{-4} $day^{-1} \cdot (\mu g/mL)^{-1}$
Γ_P	rate of killing of nCSCs by the chemotherapeutic agent	5.2 - 7.0 x 10^{-3} $day^{-1} \cdot (\mu g/mL)^{-1}$
e_C	elimination rate of the chemotherapeutic agent	49 - 124 day^{-1}

Table 1. Parameter descriptions and possible values based on Table 2 in Sigal et al. (2019). These biologically relevant ranges for each of parameter were derived using experimental data from other studies (Luo et al., 2014; Ning et al., 2012) and values in other models of cancer and immune cell growth and interactions (Gao et al., 2012; Turner & Kohandel, 2012).

Using their model, the authors reproduced data from several experiments, including from Luo et al. (2014) and Ning et al. (2012), to ensure that the model accurately represented tumor growth for tumors with and without CSCs. They then simulated the efficacy of immunotherapy and chemotherapy when used alone and together.

In this report, I will detail my replications of the model's simulations using Mathematica to confirm that the model is reproducible and accurately portrays CSC and nCSC growth and response to different treatments. I will then explain my modification of the model by introducing a Gompertz term to better reflect the long-term tumor dynamics, where tumor growth slows as it approaches a carrying capacity. Finally, I will explore how the addition of this Gompertz term impacts the model's simulations of immunotherapy's efficacy.

Breakdown of the Model

Tumor Cells

Sigal et al. (2019) mainly focused on graphing the differential equations (DEs) for S and P, which model CSC and nCSC populations, to analyze the tumor size and how it is impacted by treatments. Despite the drastic differences between CSCs and nCSCs, there are mechanisms by which they can differentiate into each other. These are captured by the 2 DEs:

$$\frac{dS}{dt} = \alpha_S S + \rho_{PS} P - \rho_{PS} S - \beta_S S T_S - \delta_S S - \Gamma_S S C$$

$$\frac{dP}{dt} = \alpha_P P + \alpha_{SP} S + 2\rho_{SP} S - \rho_{PS} P - \beta_P P T_P - \delta_P P - \Gamma_P P C \quad \textbf{(1.1)}$$

CSCs can undergo three different types of cell division: symmetric, asymmetric, and interconversion. Symmetric division happens 10-45% of the time. A CSC forms 2 new CSCs at a rate captured by α_S (a daughter cell replaces the parent cell, resulting in the exponential first term of $\frac{dS}{dt}$). Asymmetric division, where 1 CSC and 1 nCSC are formed, occurs 55-80% of the time. In the model, this occurs at a rate of α_{SP} (this only appears in the DE for P as $\alpha_{SP}S$ because the CSC population is conserved). Interconversion, where a CSC forms 2 nCSCs, happens in 0-10% of CSCs at rate ρ_{SP} (corresponding with $-\rho_{SP}S$ and $2\rho_{SP}S$ in the S and P DEs).

Depending on their characteristics, nCSCs can also undergo replication at a rate of α_P (resulting in the exponential $\alpha_P P$ term in $\frac{dP}{dt}$) or dedifferentiate back into a CSC at rate ρ_{PS}. The value of ρ_{PS} is chosen to keep the CSC population within a reasonable range, ensuring CSCs make up under 10% of the total tumor cells. This dedifferentiation process is represented by $\rho_{PS}P$ in $\frac{dS}{dt}$ (the CSCs formed) and $-\rho_{PS}P$ in $\frac{dP}{dt}$ (the nCSCs that differentiated).

The $-\beta_S S T_S$ and $-\beta_P P T_P$ terms model cancer cell death by CTCs, which occurs when CSCs and nCSCs come in contact with an activated CTC that targets them (denoted by T_S and T_P). Meanwhile, the $-\Gamma_S SC$ and $-\Gamma_P PC$ terms model killing by chemotherapy when CSCs and nCSCs encounter chemotherapeutic agents (denoted by C). There are distinct parameters for CSC and nCSC death because CSCs are far more resistant to chemotherapy.

Finally, there is a term modeling natural death for all the tumor cell, dendritic cell, and cytotoxic T-cell ODEs. Each is modeled by an exponential decay term with a δ_I parameter specific to the cell type I. However, because of CSC's ability to proliferate indefinitely, this term can sometimes be removed entirely from the equation for S.

Cytotoxic T-Cells

The DEs for activated CSC-specific and nCSC-specific CTCs (T_S and T_P) have 2 terms:

$$\frac{dT_S}{dt} = K_{T_S} T_S{}^n \frac{D_S}{S_{T_S}+D_S} - \delta_{T_S} T_S$$

$$\frac{dT_P}{dt} = K_{T_P} T_P{}^n \frac{D_P}{S_{T_P}+D_P} - \delta_{T_P} T_P \quad \textbf{(1.2)}$$

The first term represents naive CTC activation by mature DCs. At high concentrations of DCs, this becomes saturated and reaches the value of parameter $K_{T_S}T_S{}^n$or $K_{T_P}T_P{}^n$ (the saturated activation rate of CTCs multiplied by the population of CSC- or nCSC-specific naive CTCs). The other term represents the natural death rate of activated CTCs.

Dendritic Cells

Meanwhile, the DEs for mature DCs specific to CSCs or nCSCs (D_S and D_P) involve 3 terms and describe how mDCs are produced and the two ways in which they can die:

$$\frac{dD_S}{dt} = \gamma_{D_S} DS - \beta_{D_S} D_S T_S - \delta_{D_S} D_S$$

$$\frac{dD_P}{dt} = \gamma_{D_P} DP - \beta_{D_P} D_P T_P - \delta_{D_P} D_P \quad \textbf{(1.3)}$$

The first term shows how naive DCs (whose population is represented by the constant D) mature when encountering a tumor cell. The second term represents mDC death by activated CTCs because of the antigens that the mDCs are presenting. The last term represents natural death.

Chemotherapeutics

Finally, the DE modeling chemotherapeutic agents (C) has a single term modeling the clearance of these drugs from the body:

$$\frac{dC}{dt} = -e_C C \quad \textbf{(1.4)}$$

Simulations

To validate the model, I began by replicating simulations Sigal et al. performed using data from two experimental studies (Luo et al., 2014; Ning et al., 2012). These studies involved injecting mice with CSCs and nCSCs, as well as giving them immunotherapy targeting either CSCs, nCSCs, both cell types, or providing no treatment.

I first reproduced the authors' simulation of experimental data of CSC and nCSC tumor growth from experimental data in Ning et al. (2012) **(Fig. 1)**. In the experiment, varying amounts of CSCs and nCSCs were isolated and injected into opposite sides of the same immunocompetent mouse. The size of the tumors that resulted (which had both CSCs and nCSCs because of their ability to convert into each other) were monitored over time. Both studies found that the tumors started with CSCs grew much quicker and more aggressively than ones originating from nCSCs, and Sigal et al.'s models were able to capture that.

To replicate the authors' model, I focused on the DEs for S and P. I added S and P together to get the total tumor size in units of mm^3 (assuming there are 10^5 tumor cells per mm^3, as Sigal et al. did). In the graphs, day 0 corresponds with when the tumor cells took root and induced a tumor in the mouse models.

I started by modeling the growth of a tumor without treatment by varying the initial CSC and nCSC populations and setting the population of CTCs, DCs, and chemotherapeutic agents to 0. I first reproduced modeling of tumor size after inoculation with 50,000 CSCs or nCSCs **(Fig. 1a)**. I used host-specific parameters (which depend on the tumor microenvironment and cancer type in each individual host): $\alpha_S = 0.5$, $\delta_S = 0.2$, $\alpha_P = 0.25$, $\delta_P = 0.2$, $\rho_{SP} = 0.15$, $\alpha_{SP} = 1.8$, and $\rho_{PS} = 0.00053$. These values were selected based on the ones used in Fig 2 of Sigal et al. (2019) and the possible ranges for parameters, which can be found, along with their units, in **Table 1**. I also modeled tumor size with initial populations of 5,000, 10,000, and 20,000 CSCs or nCSCs with $\alpha_S = 0.51$, $\delta_S = 0.2$, $\alpha_P = 0.24$, $\delta_P = 0.2$, $\rho_{SP} = 0.15$, $\alpha_{SP} = 1.6$, and $\rho_{PS} = 0.00018$ **(Fig. 1b)**.

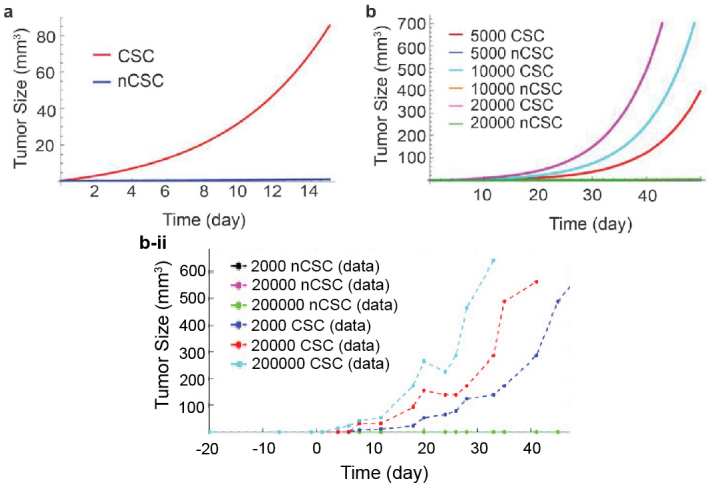

Figure 1. Tumor growth over time with different initial populations of CSCs and nCSCs, with day 0 corresponding to when tumors took root and started growing. **(a)** Initial population of 50,000 CSCs or nCSCs. **(b)** Initial population of 5,000, 10,000, and 20,000 CSCs or nCSCs. Initial populations in this simulation were selected to compare with **(b-ii)** mean tumor size measured experimentally in Figure 2b in Ning et al. (2012) with initial population of 2,000, 20,000, and 200,000 CSCs or nCSCs, plot from Figure 2cii in Sigal et al. (2019).

This simulation successfully captured how CSCs grow far more aggressively than nCSCs, with just 5,000 CSCs being sufficient to form a tumor of substantial size over t = 50 days **(Fig. 1b)**. Furthermore, this simulation showed that varying the size of the initial nCSC population (even with a tenfold increase) doesn't create a significant difference in the size of the resulting tumor **(Fig. 1a, 1b)**. However, while the experimental data in **Figure 1b-ii** shows tumor growth slowing as it is limited by nutrient availability and reaches a carrying capacity, even in tumors starting with far more CSCs, the simulated tumor populations in **Figure 1b** continue to grow exponentially.

Next, I reproduced a model of tumor size after treatments with DCs or CTCs using in vivo experimental data from Figure 4 in Ning et al. (2012) **(Fig. 2)**. Mice were injected with a combination of CSCs and nCSCs and received either immunotherapy targeting CSCs, nCSCs, both cell types (mixed treatment), or no treatment at all. Most of the DCs and CTCs were applied over multiple inoculations before the tumor cells took root in the mice (modeled as day 0), with the treatment schedule shown in **Figure 2a**. I simulated the DC and CTC populations prior to day 0 and used those results as the initial conditions in the system of 7 DEs.

I started by modeling treatment with DCs **(Fig. 2b)**. In the experiment, $3x10^6$ DCs were applied to a mouse over three injections that occurred 22, 15, and 8 days prior to day 0, when a tumor with 10% CSCs and 10^5 total cells took root. For the treatments that targeted CSCs and nCSCs, all of the DCs were either CSC- or nCSC-specific. For the mixed treatment, 10% of the DCs were CSC-specific, and the rest targeted nCSCs, corresponding with the composition of the initial tumor cell population. I used parameters $\alpha_S = 0.7$, $\delta_S = 0.1$, $\alpha_P = 0.2$, $\delta_P = 0.2$, $\rho_{SP} = 0.2$, $\alpha_{SP} = 3.2$, and $\rho_{PS} = 0$ based on the values Sigal et al. (2019) selected.

For CTCs, I modeled how a total of $3x10^6$ CTCs were applied 7 days before, the day of, and 7 days after a tumor with 10^5 cells (5% CSCs) took root **(Fig. 2c)**. Much like with the DCs, treatment consisted of CSC-specific CTCs, nCSC-specific CTCs, or a mix of both (with 5% targeting CSCs). I used parameters $\alpha_S = 0.71$, $\delta_S = 0.2$, $\alpha_P = 0.3$, $\delta_P = 0.2$, $\rho_{SP} = 0.24$, $\alpha_{SP} = 2.8$, and $\rho_{PS} = 0.00013$.

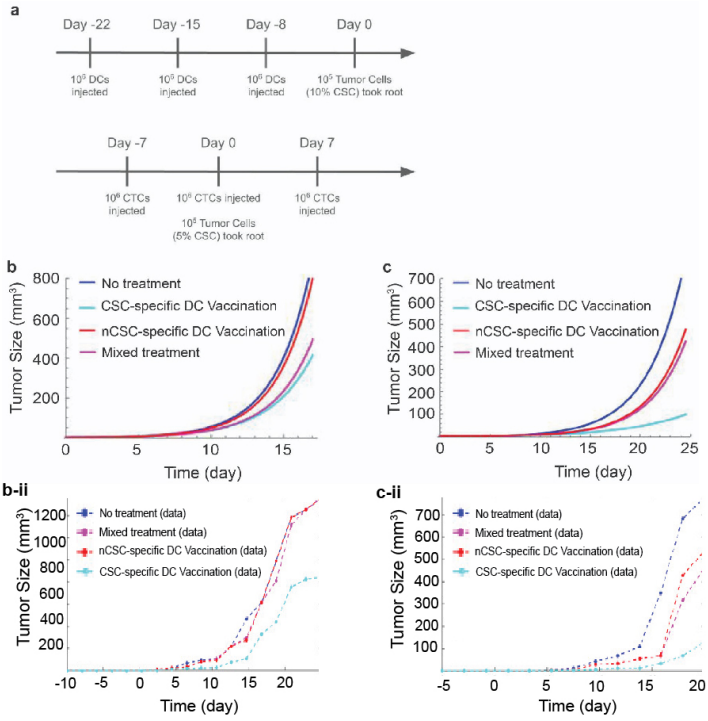

Figure 2. Tumor growth over time after various applications of DCs or CTCs targeting CSCs, nCSCs, both cell types (mixed treatment), or no treatment at all. **(a)** Timeline of treatment with immunotherapy and tumor cells. **(b)** A tumor with 10% CSCs treated with various applications of DCs. Simulation values selected to compare with **(b-ii)** mean tumor size measured experimentally in Figure 4d in Ning et al. (2012), plot from Figure 3b-ii in Sigal et al. (2019). **(c)** A tumor with 5% CSCs treated with various applications of CTCs. Simulation values selected to compare with **(c-ii)** mean tumor size measured experimentally in Figure 4c in Ning et al. (2012), plot from Figure 3c-ii in Sigal et al. (2019).

In **Figure 2**, this model captures the performance of these different treatment regimens relative to each other and to no treatment. The simulation also confirms that immunotherapy targeting CSCs is more effective than treatments targeting nCSCs or both cell types. However, the solution curves modeling tumor growth rates grew far more aggressively than the experimental data, which displays clear sigmoidal growth, with tumor growth slowing and beginning to approach a carrying capacity 20 days after the tumors took root **(Fig. 2b-ii, 2c-ii)**. As a result, Equation 1 failed to model the long-term behavior of the tumors because it assumes tumors obey Malthusian, or simple exponential growth.

Model Modifications

Knowing that tumor growth in vivo is limited by oxygen and nutrient availability, making Malthusian growth unrealistic, I decided to modify the equations for S and P so it can simulate tumors with sigmoidal growth and approaching a carrying capacity. However, the model needed to identify a carrying capacity using the initial tumor population, cell growth rates, and death rates. To account for tumors' slowing growth as they near a carrying capacity, I replaced the exponential Malthusian growth terms with Gompertz terms, which better capture long-term tumor dynamics and allow the sigmoidal growth to approach a carrying capacity without explicitly setting its value. This flexibility is particularly useful for modeling tumor growth.

I selected a Gompertz term to replace the Malthusian terms modeling cell division ($\alpha_S S$ and $\alpha_P P$) and natural death ($-\delta_S S$ and $-\delta_P P$) and got a modified system of the 7 ODEs:

$$\frac{dS}{dt} = \delta_S S \ln\left(\frac{S}{\theta_S}\right) + \rho_{PS} P - \rho_{PS} S - \beta_S S T_S - \delta_S S - \Gamma_S S C$$

$$\frac{dP}{dt} = \delta_P P \ln\left(\frac{P}{\theta_P}\right) + \alpha_{SP} S + 2\rho_{SP} S - \rho_{PS} P - \beta_P P T_P - \delta_P P - \Gamma_P P C$$

$$\frac{dT_S}{dt} = K_{T_S} T_S{}^n \frac{D_S}{S_{T_S}+D_S} - \delta_{T_S} T_S$$

$$\frac{dT_P}{dt} = K_{T_P} T_P{}^n \frac{D_P}{S_{T_P}+D_P} - \delta_{T_P} T_P \qquad \textbf{(2)}$$

$$\frac{dD_S}{dt} = \gamma_{D_S} D S - \beta_{D_S} D_S T_S - \delta_{D_S} D_S$$

$$\frac{dD_P}{dt} = \gamma_{D_P} D P - \beta_{D_P} D_P T_P - \delta_{D_P} D_P$$

$$\frac{dC}{dt} = -e_C C$$

The Gompertz terms for S and P, $\delta_S S \ln\left(\frac{S}{\theta_S}\right)$ and $\delta_P P \ln\left(\frac{P}{\theta_P}\right)$, incorporate tumor cell growth and death rates, as well as the initial population of each type of cancer cell, and are derived from Tier (2003) and (Norton, 1988). The new parameter θ_I is defined as follows for cells of type I (S or P):

$$\theta_I = I_0 e^{\alpha_I / \delta_I} \qquad \textbf{(2.1)}$$

Here, I_0 is a positive, nonzero value that represents the initial population of S or P. The definitions of parameters α_S, α_P, δ_S, and δ_P remain the same.

Since Sigal et al. only provided values for the rate of natural increase, or $\alpha_S - \delta_S$ and $\alpha_P - \delta_P$, I selected a maximum tumor size of 500-700 mm^3 to fit the carrying capacity observed in the empirical data from Ning et al. (2012). This upper limit is based on experimental data and represents an empirical assumption. Keeping all other parameter values constant with the Malthusian version of each simulation, I varied α_S, α_P, δ_S, and δ_P within their biologically relevant ranges to select the optimal values for reproducing experimental data while ensuring the tumor populations approached the observed carrying capacity.

Results

I first used my modified system of ODEs to model tumor growth in the absence of any treatments. I also tried to identify whether the percentage of CSCs making up a tumor creates a significant difference in its growth or whether it can reach the same carrying capacity. Since initial conditions for both CSCs and nCSCs must be greater than 0, I modeled the growth of 1%, 5%, and 10% CSC tumors originating from 50,000 cancer cells over t = 150 days **(Fig. 3)**. I used host-specific parameters $\alpha_S = 0.33$, $\delta_S = 0.075$, $\alpha_P = 0.03$, $\delta_P = 0.025$, $\rho_{SP} = 0.15$, $\alpha_{SP} = 1.8$, and $\rho_{PS} = 0.00053$.

These simulated tumors exhibit Gompertzian growth, starting with exponential growth that then flatten out as they begin to approach an equilibrium of 550 mm^3 at their carrying capacity at around t = 120 days. This matches the trend of the experimental data, especially over longer periods of time. Despite the different percentages of CSCs making up the three tumors, they exhibit similar growth before nearing the carrying capacity at about the same time.

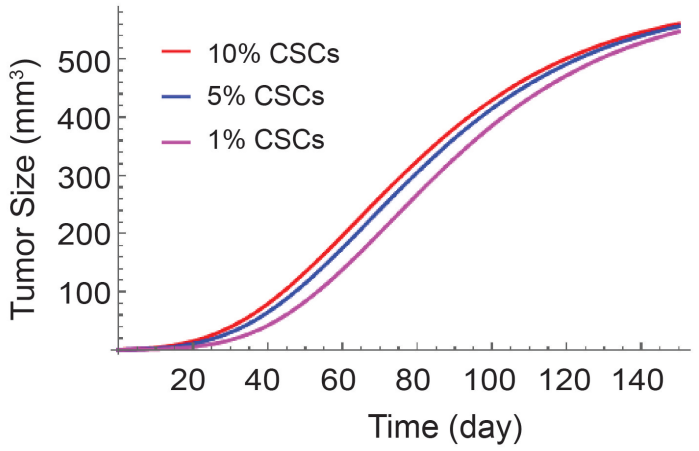

Figure 3. Tumor growth over time using a Gompertz model with an initial population of 50,000 tumor cells, with 1%, 5%, and 10% being CSCs.

I then modeled tumor growth after treatment with DCs and CTCs using this modified system of ODEs to identify whether Gompertzian growth impacts the efficacy of immunotherapy. Parameters ρ_{SP}, α_{SP}, and ρ_{PS}, which model the rate of transitions between CSCs and nCSCs, were kept constant for DCs and CTCs from their counterparts in **Figures 2b** and **2c**. I identified parameters $\alpha_S = 0.675$, $\delta_S = 0.075$, $\alpha_P = 0.04$, and $\delta_P = 0.04$ to model treatment with DCs in **Figure 4a** and $\alpha_S = 0.67$, $\delta_S = 0.06$, $\alpha_P = 0.16$, and $\delta_P = 0.06$ to model the use of CTCs in **Figure 4b**. Using the same dosage and initial conditions as I detailed in **Figure 2a**, I obtained the solution curves shown in **Figure 4**:

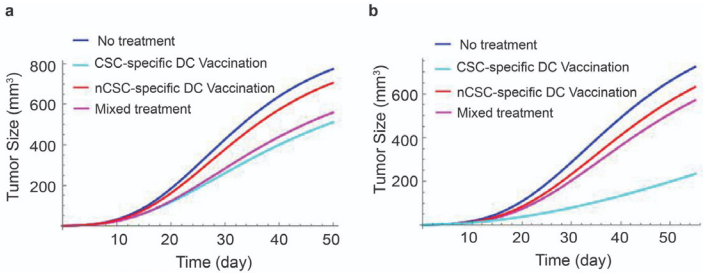

Figure 4. Tumor growth over time after various applications of DCs or CTCs targeting CSCs, nCSCs, both cell types, or no treatment using a Gompertz model. **(a)** A tumor with 10% CSCs treated with various applications of DCs. **(b)** A tumor with 5% CSCs treated with various CTC applications.

Figure 4 shows how the improved system of ODEs qualitatively captures the relative efficacy of the various treatments, comparing each treatment to one another as well as to the no-treatment control. Once again, immunotherapy targeting CSCs performs the best. The curves all show sigmoid Gompertzian growth and flatten out at about t = 50 days at different values, matching with the experimental data **(Fig. 2b-ii, 2c-ii)** and showing more realistic tumor growth than the original model's simulations (Equation 1) **(Fig. 2b, 2c).** However, if treatment is not continued, the modified model predicts that all of these solution curves will eventually converge at a carrying capacity of about 800 mm^3 (the value the no treatment curves are currently at).

Discussion

In summary, this report presents a modified system of 7 ODEs that models Gompertzian tumor growth and the effects of immunotherapy when used alone and together with chemotherapy, serving as an improvement upon Sigal et al.'s model of exponential tumor growth. This modified model is valuable because it recognizes that there are limits to tumor growth in vivo because of the finite amount of resources available and can simulate sigmoidal growth, with tumor growth slowing as the tumor reaches an equilibrium at its carrying capacity. This allows the solution curves in the model to exhibit much more realistic long-term growth. Moreover, if the growth and natural death rates of CSCs and nCSCs, along with the values of the other host-specific variables governing the conversions between CSCs and nCSCs are known, this model can predict the eventual size of the tumor.

There are a few improvements that could be made to this model. While the model simulated most of the equilibrium values that the tumors in the experimental data approached after receiving immunotherapy or no treatment, there are a few discrepancies. For example, tumor growth in mice receiving CSC-specific immunotherapy was significantly lower in the experimental data than what the model predicts. This can in part be attributed to a difference in the number of tumor cells injected into the mouse and how many actually took root. Of course, tuning specific parameter values, such as β_S, which governs the death rate of CSCs in response to CTCs (and DCs, by extension), could improve the model. This is especially because Sigal et al. set β_S and β_P equal in their model **(Table 1)**, assuming that CTCs are equally effective at killing CSCs and nCSCs, contrary to what the experimental data suggests. Additionally, the model currently makes the simplifying assumptions that activated CTCs will only target mature DCs and tumor cells with the same type of antigen, and chooses not to account for mechanisms protecting mature DCs from such attacks. Modifying the model to consider these could be another point of future studies.

Moreover, it took the modified model two to three times as long to approach equilibrium values: solution curves took about 50 days after tumors took root to do so while the tumors in the experimental data did so in about 15 to 25 days. This difference could be attributed to a need to further tune parameter values and could be a point of future studies.

Currently, this model is unable to simulate initial tumor populations where either CSCs or nCSCs are 0. However, most tumors are heterogeneous and include both CSC and nCSC populations. CSCs typically make up under 10% of a tumor and can differentiate into other cell types, making it unlikely for a tumor to be entirely composed of CSCs. Moreover, tumors composed entirely of nCSCs do not grow aggressively enough to reach a carrying capacity on the relatively short timescale of a few weeks to a few months that I modeled, as seen in **Figure 1**. This makes the case where a tumor is initially entirely CSCs or nCSCs and needs to be simulated using Gompertzian growth unlikely. However, extending the model to simulate this case is another important and interesting point of future study.

This modified model has the potential to provide valuable insights into the potential efficacy of cancer treatments. By incorporating host-specific parameters and tumor composition, it can simulate the long-term behavior of tumors. Additionally, modeling interactions between cancer cells, immunotherapy, and chemotherapeutic agents may provide insights into the optimal timing and efficacy of treatments.

References

Galassi, C., Musella, M., Manduca, N., Maccafeo, E., & Sistigu, A. (2021). The Immune Privilege of Cancer Stem Cells: A Key to Understanding Tumor Immune Escape and Therapy Failure. *Cells, 10*(9), 2361. https://doi.org/10.3390/cells10092361

Gao, X., McDonald, J. T., Hlatky, L., & Enderling, H. (2012). Acute and fractionated irradiation differentially modulate glioma stem cell division kinetics. *Cancer Research, 73*(5), 1481. https://doi.org/10.1158/0008-5472.CAN-12-3429

Goldman, A., Majumder, B., Dhawan, A., Ravi, S., Goldman, D., Kohandel, M., Majumder, P. K., & Sengupta, S. (2015). Temporally sequenced anticancer drugs overcome adaptive resistance by targeting a vulnerable chemotherapy-induced phenotypic transition. *Nature Communications, 6*(1), 6139. https://doi.org/10.1038/ncomms7139

Jhunjhunwala, S., Hammer, C., & Delamarre, L. (2021). Antigen presentation in cancer: Insights into tumour immunogenicity and immune evasion. *Nature Reviews Cancer, 21*(5), 298–312. https://doi.org/10.1038/s41568-021-00339-z

Luo, H., Zeng, C., Fang, C., Seeruttun, S. R., Lv, L., & Wang, W. (2014). A New Strategy Using ALDHhigh-CD8+T Cells to Inhibit Tumorigenesis. *PloS One, 9*(8), e103193. https://doi.org/10.1371/journal.pone.0103193

Ma, J. Z.-I., Lim, S. N., Qin, J. S., Yang, J., Enomoto, N., Ruedl, C., & Ronchese, F. (2012). Murine CD4+ T cell responses are inhibited by cytotoxic T cell-mediated killing of dendritic cells and are restored by antigen transfer. *PloS One, 7*(5), e37481. https://doi.org/10.1371/journal.pone.0037481

Mpekris, F., Baish, J. W., Stylianopoulos, T., & Jain, R. K. (2017). Role of vascular normalization in benefit from metronomic chemotherapy. *Proceedings of the National Academy of Sciences, 114*(8), 1994–1999. https://doi.org/10.1073/pnas.1700340114

Mpekris, F., Voutouri, C., Baish, J. W., Duda, D. G., Munn, L. L., Stylianopoulos, T., & Jain, R. K. (2020). Combining microenvironment normalization strategies to improve cancer immunotherapy. *Proceedings of the National Academy of Sciences, 117*(7), 3728–3737. https://doi.org/10.1073/pnas.1919764117

Ning, N., Pan, Q., Zheng, F., Teitz-Tennenbaum, S., Egenti, M., Yet, J., Li, M., Ginestier, C., Wicha, M. S., Moyer, J. S., EPPrince, M., Xu, Y., Zhang, X.-L., Huang, S., Chang, A. E., & Li, Q. (2012). Cancer stem cell vaccination confers significant anti-tumor immunity. *Cancer Research, 72*(7), 1853. https://doi.org/10.1158/0008-5472.CAN-11-1400

Norton, L. (1988). A Gompertzian model of human breast cancer growth. *Cancer Research, 48*(24 Pt 1), 7067–7071.

Robertson-Tessi, M., El-Kareh, A., & Goriely, A. (2012). A mathematical model of tumor–immune interactions. *Journal of Theoretical Biology, 294*, 56–73. https://doi.org/10.1016/j.jtbi.2011.10.027

Sigal, D., Przedborski, M., Sivaloganathan, D., & Kohandel, M. (2019). Mathematical modelling of cancer stem cell-targeted immunotherapy. *Mathematical Biosciences, 318*, 108269. https://doi.org/10.1016/j.mbs.2019.108269

Tier, C. (2003). Biomathematics- Gompertz Equation. https://homepages.math.uic.edu/~tier/Math419/Tumor/Notes/gompertz.html

Turner, C., & Kohandel, M. (2012). Quantitative approaches to cancer stem cells and epithelial-mesenchymal transition. *Seminars in Cancer Biology, 22*(5–6), 374–378. https://doi.org/10.1016/j.semcancer.2012.04.005

Wilkie, K. P., & Hahnfeldt, P. (2013). Mathematical models of immune-induced cancer dormancy and the emergence of immune evasion. *Interface Focus, 3*(4), 20130010. https://doi.org/10.1098/rsfs.2013.0010

Wu, B., Shi, X., Jiang, M., & Liu, H. (2023). Cross-talk between cancer stem cells and immune cells: Potential therapeutic targets in the tumor immune microenvironment. *Molecular Cancer, 22*(1), 38. https://doi.org/10.1186/s12943-023-01748-4